JOURNAL OF CHEMICAL INFORMATION AND MODELING

Article

pubs.acs.org/jcim

Molecular Mechanism of Selective Binding of Peptides to Silicon Surface

Sathish Kumar Ramakrishnan,[†,‡] Marta Martin,[†,‡] Thierry Cloitre,[†,‡] Lucyna Firlej,[†,‡] and Csilla Gergely*[,†,‡]

[†]Université Montpellier 2, Laboratoire Charles Coulomb UMR 5221, F-34095 Montpellier, France

[‡]CNRS, Laboratoire Charles Coulomb UMR 5221, F-34095 Montpellier, France

Supporting Information

ABSTRACT: Despite extensive recent research efforts on material-specific peptides, the fundamental problem to be explored yet is the molecular interactions between peptides and inorganic surfaces. Here we used computer simulations (density functional theory and classical molecular dynamics) to investigate the adsorption mechanism of silicon-binding peptides and the role of individual amino acids in the affinity of peptides for an n-type silicon (n^+-Si) semiconductor. Three silicon binding 12-mer peptides previously elaborated using phage display technology have been studied. The peptides' conformations close to the surface have been determined and the best-binding amino acids have been identified. Adsorption energy calculations explain the experimentally observed different degrees of affinity of the peptides for n^+-Si. Our residual scanning analysis demonstrates that the binding affinity relies on both the identity of the amino acid and its location in the peptide sequence.

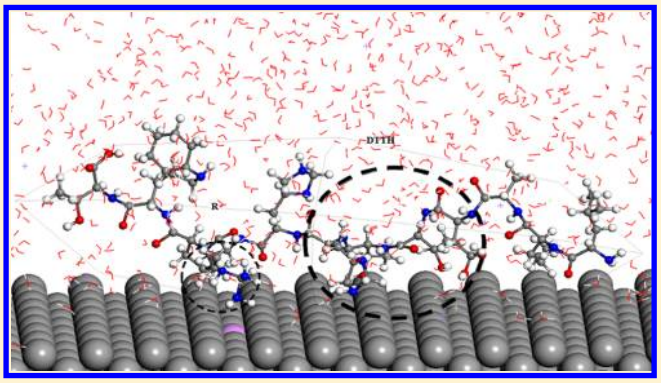

INTRODUCTION

Nature handles biomolecules to form composite materials with remarkable properties such as teeth,[1] sea shells,[2] bones, and cartilage[3] under strict biological mediation and control. In vivo, to control the formation of organized nanostructures under ambient conditions, proteins and peptides undergo self-assembly processes driven by specific molecular recognition events.[4] Therefore, peptides with exquisite recognition functions toward various targets can be exploited to mimic this behavior,[5] control nanoparticle growth,[6] and create smart sensing devices.[7] The phage display technique has been extensively used during past decade to select from a pool of billions peptides those that are specific and/or reveal affinity for a given target and strongly adhere to a substrate. Several polypeptides presenting high binding affinities toward metals,[8,9] oxides,[10] polymers,[11] carbon nanotubes,[12] and inorganic semiconductors[13−16] were recently identified. They offer an alternative way of surface modification that is complementary to grafting chemistry. They can act as nanosized affinity linkers that allow controlled recognition between the surface and biomolecules at the atomic level.[16] The surface-specific adhesion of peptides enables controlled placement of biomolecules on various nano/micropatterned surfaces.[14,16] Peptide-mediated surface functionalization was also found to preserve enzyme activity and native secondary structure upon adsorption.[17]

Although substantial progress in engineering smart functional materials using adhesion peptides was foreseen, progress in the field remains limited because of the still-open questions in understanding peptide−surface interactions at the atomic level. Knowledge of the driving force by which peptides recognize the surface might pave the way toward promising applications in programmed materials synthesis, precise biopatterning, preservation of the activity of adsorbed biomolecules, and biosensor development.

Peptides are generally flexible and adopt multiple conformations in solution, with a high concentration of inactive conformations.[18] The sequence of amino acids in a peptide plays a crucial role in its capacity to reach the optimal conformation for surface adhesion.[19] Peptide−surface interactions are driven by a combination of polar and van der Waals interactions, electrostatic forces, and hydrogen bonds, which collectively approach the strength of a covalent bond. The charge-driven binding of homopeptides to inorganic surfaces was investigated experimentally.[20] It was found that positively charged polylysine, polyarginine, and polyhistidine strongly adsorb on the negatively charged SiO_2 surface. However, negatively charged polyglutamic acid also binds strongly to SiO_2, whereas polyaspartic acid (with features similar to those of polyglutamic acid) does not adhere to the SiO_2 surface. This suggests that the mechanism of peptide−surface adhesion involves phenomena that go beyond charge transfer between amino acids and the substrate. Recently, Puddu and Perry[21] demonstrated evidence of hydrophobic interactions between

Received: April 30, 2014
Published: June 9, 2014

dx.doi.org/10.1021/ci500260v | J. Chem. Inf. Model. 2014, 54, 2117−2126

Scheme 1. Rational Modeling Approach To Understand Peptide−Semiconductor Interactions[a]

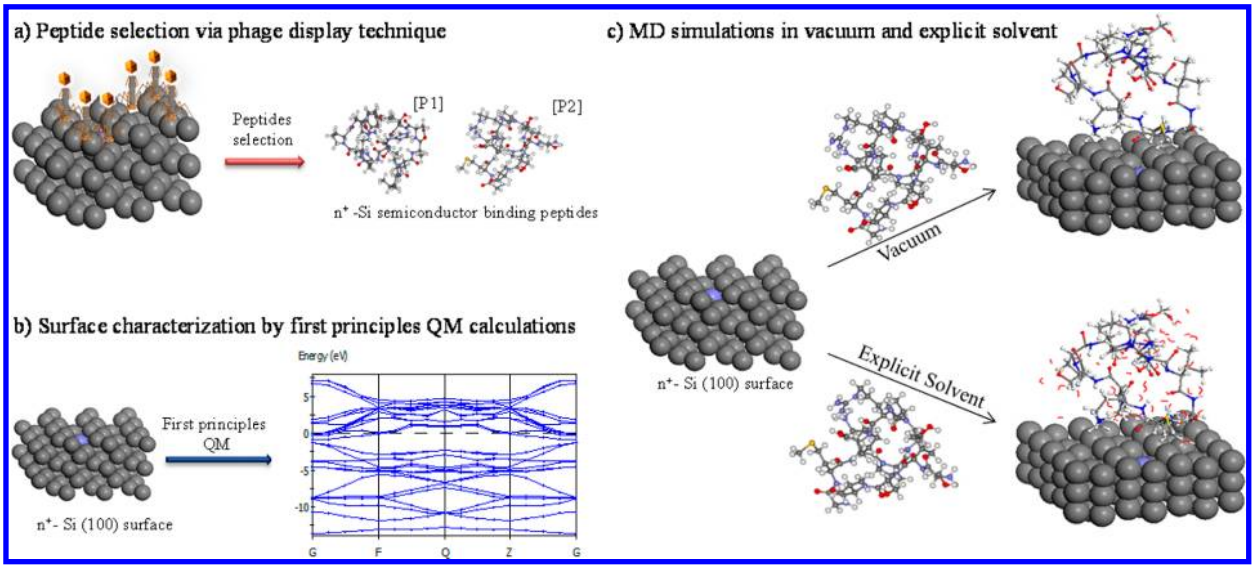

[a]The three steps are as follows: (a) elaboration of the structures of n^+-Si-binding peptides previously selected using the phage display technology; (b) first-principles quantum-mechanical (QM) calculations to determine the properties of the doped n^+-Si(100) surface; and (c) molecular dynamics (MD) calculations to reveal the interactions of the peptides and n^+-Si(100) under vacuum and explicit-solvent conditions.

silica nanoparticles and peptides with heterogeneous physiochemical properties. They showed that highly charged peptides bind through electrostatic interactions whereas neutral or negatively charged peptides bind through non-Coulombic interactions. Also, we reported that peptides having high net charge show less affinity for silicon surfaces than nonpolar peptides.[22] In view of all this information, it is clear that more investigation is needed to understand surface−peptide interactions at the molecular level.

Theoretical studies aiming to elucidate the mechanism of interactions between peptides and surfaces are scarce. Recent efforts to bring to light the theory of peptide−substrate recognition processes are limited to metal[23,24] and metal oxides.[25] Density functional theory (DFT) was employed to investigate the adsorption of individual amino acids on metallic surfaces.[26,27] Exploring the interactions of peptides with semiconductors is particularly challenging as no accurate force-field parameters are available and the distribution of charge carriers should be taken into account. In the present work, we developed a new, efficient, multistep computational approach for exploring the interactions between peptides and silicon. Silicon is the basic semiconductor used for mass production of a large variety of electronic devices. For all such applications, control of the silicon surface chemistry is crucial. The electronic functionality of Si-based devices can be enlarged by coupling biomolecules to silicon; however, only modest binding affinities have been achieved by classical grafting chemistry.[28−31] We recently reported enhanced grafting of biomolecules on silicon surfaces via a peptide functionalization route, using peptides showing high affinities for n^+-Si, p-Si, and p^+-Si semiconductors[22] that were preselected with the phage display technique.

The positive output of this experimental work motivated us to investigate the microscopic mechanism of binding of experimentally selected adhesion peptides on Si surfaces. Though the combinatorial phage display technique demonstrated the surface recognition capacity of peptides, the method does not provide information on the main binding sequences within the peptide or on the underlying interactions. Theoretical computational tools might provide valuable insight into these issues, opening the way to tailor peptides' properties according to the desired application. As recently reported,[32] the preferential attachment of peptides toward materials (e.g., platinum) can be explained by means of molecular dynamics (MD) simulations. MD calculations allow the identification of those amino acids in the peptide sequence that bind the best to the substrate and provide the peptide conformation upon adsorption.[33] Both pieces of information are essential when optimal strategies for controlled immobilization of biomolecules on surfaces are prospected and when peptides are used for bottom-up self-assembly of nanostructures. Recent developments made by incorporating accurate Lennard-Jones parameters in widely employed force fields such as AMBER, CHARMM, COMPASS, CVFF, and PCFF tackle prior pitfalls in modeling of silica interfaces.[34] We employed a similar approach by using classical MD simulations to study the adsorption mechanisms of peptides and to calculate the energies of their binding to silicon in vacuum and in aqueous solution.[22]

■ RESULTS AND DISCUSSION

We employed a rational modeling approach to understand the interactions by which peptides recognize semiconductors. The model surface here is n-type silicon [n^+-Si(100); Scheme 1]. Our methodology consists of three main modeling steps: (a) preparation of experimentally evolved peptide structures (random-coil and local-minimum conformations), (b) simulation of the n^+-Si doping process and surface characterization by first-principles calculations under the framework of DFT, and (c) classical MD simulations to compute interaction energies between peptides and Si in vacuum and explicit solvent.

Our calculations address the adsorption of three 12-mer peptides that were previously selected via phage display technology:[22] SVSVGMKPSPRP (**P1**) and LLADTTHHRPWT (**P2**) showing high affinity for n^+-type Si and SPGLSLVSHMQT (**P3**) selected as an adhesion peptide for p^+-type Si. Peptides **P1** and **P2** have different levels of affinity for n^+-Si, display no sequence similarity, and have distinct physicochemical properties (Table 1). At neutral pH, **P1**[22] bears a net charge of +2, while **P2**

dx.doi.org/10.1021/ci500260v | J. Chem. Inf. Model. 2014, 54, 2117−2126

Table 1. Sequence and Physicochemical Properties[a] of Three Peptides Exhibiting High Affinity for Silicon As Obtained by the Phage Display Technique[22]

peptides	surface	net charge	GRAVY[b]	II[c]
SVSVGMKPSPRP (**P1**)	n^+-Si	+2	−0.475	58.24
LLADTTHHRPWT (**P2**)	n^+-Si	0.2	−0.800	−9.31
SPGLSLVSHMQT (**P3**)	p^+-Si	0.1	0.158	39.50

[a]The property values were calculated using the Innovagen peptide property calculator at http://www.innovagen.com and the ProtParam tool at http://expasy.org. [b]The grand average of hydropathicity (GRAVY)[35] is defined as the sum of the hydropathy values of all of the amino acids divided by the number of residues in the peptide. The larger the GRAVY value, the more hydrophobic is the peptide. [c]II is the instability index of the peptide. For stable peptides, II < 40, while for unstable peptides, II > 40.

is a neutral peptide. **P3** is also a rather neutral peptide selected for its strong affinity for p^+-type Si and is employed here as a negative control peptide for the n^+-type Si. We expect that binding of **P2** and **P3** to Si is mainly guided through non-Coulombic interactions regardless of surface charge. We note also that the instability index of peptide **P1** is very high, contrary to that of **P2**, indicating that **P2** is a highly stable peptide in comparison with the instable **P1**.

It is clear that the nature of the surface and its charge also have a large influence on peptide binding. When phage display is used to select affinity peptides for various materials, the native oxides formed on the surfaces are removed by appropriate chemical etching. Whaley et al.[14] published the pioneering work on the elaboration of adhesion peptides for various semiconductors through phage display technology after proper chemical etching of the targets, ensuring the least oxide on the surface. Silicon surfaces are prone to form an oxide layer when they are exposed to air under ambient conditions, and hence, a HF/H_2O mixture was used to etch the surface, leading to hydride-terminated surfaces.[14,22] It is well-known that H-terminated Si surfaces (dihydride and monohydride SiH) are very similar to those of Si(100) and are reasonably stable in air as well as in organic solvents.[36,37] As here we are performing a theoretical study of the adsorption of experimentally found peptides in our model system, we mimic the experimental conditions used to elaborate them by phage display technology: peptide adhesion is simulated in phosphate-buffered saline (PBS) solution (130 mM) at pH 7, and the substrate is represented as a hydrogen-terminated silicon surface (corresponding to n^+-type Si before oxide layer formation).

Computing Peptide Structures in Bulk. The secondary structures of peptides **P1**−**P3** are not available in the protein database. The sequences of these peptides are also too short for their structures to be generated on available secondary structure prediction servers such as JPRED or PredictProtein. Hence, for each peptide, we built an atomistic model with various backbone conformations (random coil, helix, extended) in Hyperchem[38] and Accelrys Discovery Studio Visualizer 3.5. A conformational search module program was used to generate several peptide conformations in vacuum by varying the dihedral angles. Ideally, molecules spontaneously try to reorganize to minimize their potential energy. Therefore, out of the generated peptide structures, the lowest-energy conformation was considered as a local minimum state for MD simulations.[19] However, as the secondary structure prediction program SOPMA indicated that each peptide sequence was rich in random coils, both random-coil and the generated minimum-energy conformations were considered as starting geometries for MD calculations. Each peptide was solvated under explicit solvent conditions, and its energy was minimized via a conjugate-gradient method in CHARMM 27 force field calculations until the convergence of the root-mean-square (RMS) gradient (0.001 kcal mol^{-1} $Å^{-1}$).[39] Typical random-coil and local-minimum conformation structures of peptides **P1**−**P3** are presented in Figure 1.

Surface Model of the n-Type Si Semiconductor. The presence of charge carriers in a semiconductor plays a

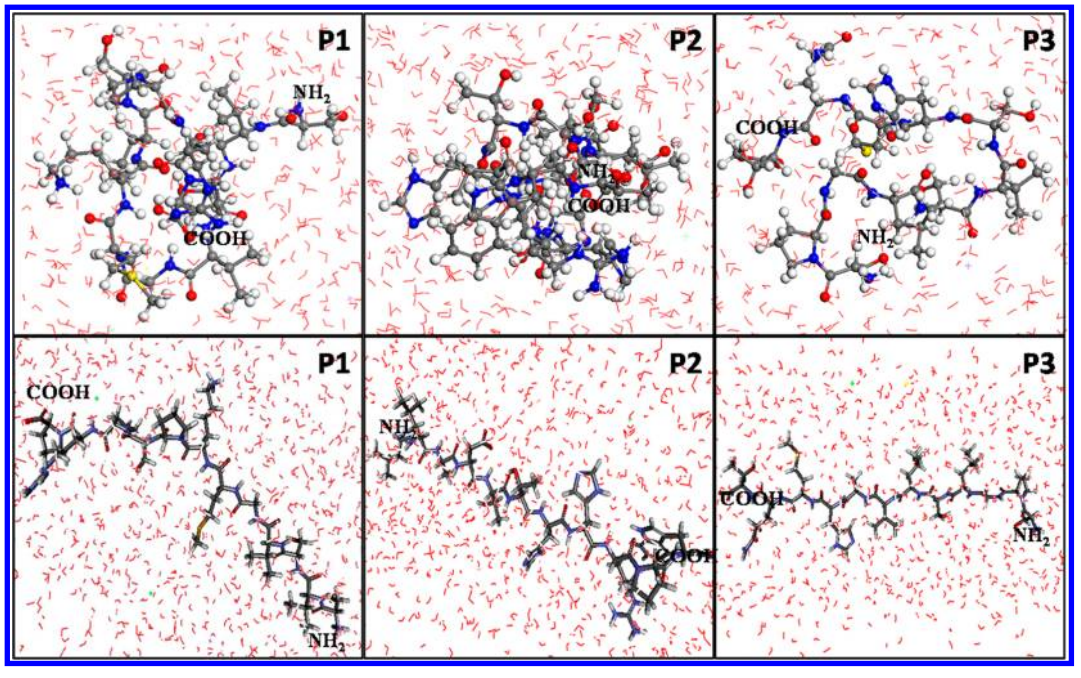

Figure 1. Snapshots of the initial conformations of the peptides SVSVGMKPSPRP (**P1**), LLADTTHHRPWT (**P2**), and SPGLSVSHMQT (**P3**) in PBS solution (137 mM) at pH 7. The top row shows local-minimum conformations, and the bottom row shows random-coil conformations.

dx.doi.org/10.1021/ci500260v | J. Chem. Inf. Model. 2014, 54, 2117−2126

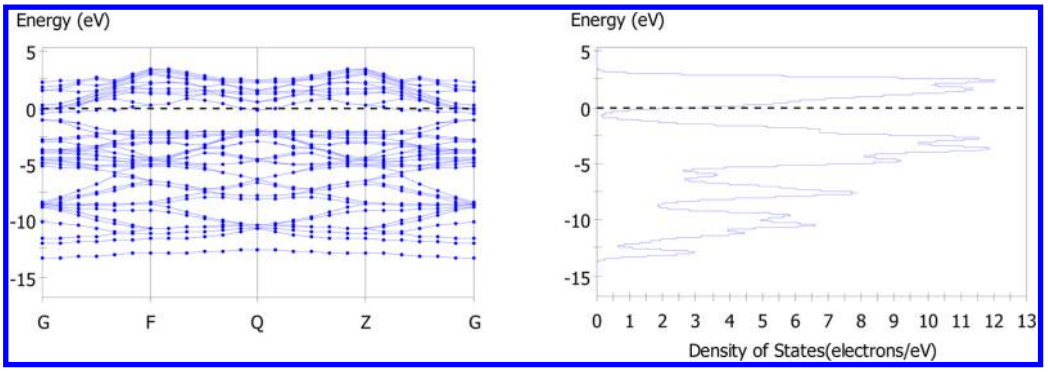

Figure 2. Computed band structure (left) and total density of states (right) of P-doped silicon along the high-symmetry lines and points G (0, 0, 0), F (0, $^1/_2$, 0), Q (0, $^1/_2$, $^1/_2$), and Z (0, 0, $^1/_2$) in the Brillouin zone. The Fermi level is indicated by the dashed line and set at zero energy.

predominant role in peptide adsorption because they contribute to charge transfer. To mimic the experimental conditions, we constructed an n^+-type (phosphorus-doped) Si semiconductor surface by replacing some Si atoms with phosphorus atoms within a Si supercell. First-principles quantum-mechanical (QM) calculations were employed to explore the properties of both undoped and phosphorus-doped (n^+-type) silicon. For the peptide adsorption studies on Si, we employed the consistent valence force field (CVFF). CVFF, like most force fields, does not contain parameters for inorganic elements; hence, we parametrized it for Si. QM calculations are more accurate for investigating interface systems but are rather computationally expensive. Semiempirical models overcome this limitation and can be applied with good accuracy for large systems by incorporation of appropriate Lennard-Jones parameters, making them suitable to study bioinorganic interfaces.

Silicon crystallizes as a face-centered cubic (fcc) cubic crystal (space group *Fd*3*m*) in which each atom has four neighbors in a unit cell. The experimental equilibrium lattice constants and their theoretical values calculated by geometry optimizations are very similar (5.43 vs 5.482 Å). The calculated band gap (0.66 eV) is smaller than the measured experimental value (1.11 eV). A scissor operator[40] of 0.45 eV was applied to equalize the theoretical and experimental band gap values. To simulate the n^+-type silicon, we constructed a $2 \times 1 \times 1$ supercell in which one Si atom was substituted by a P atom. P doping leads to significant variation of the band structure (Figure 2) compared with the intrinsic silicon band structure (Figure S1 in the Supporting Information). The calculated partial densities of states of the undoped and P-doped Si (Figure S2 in the Supporting Information) show the contribution of phosphorus atoms and indicates that the conduction band is mainly dominated by p orbitals. The computed band structure and density of states of the doped Si indicate that both the valence and conduction bands are located at the G point, which is the fingerprint of the semiconductor. We also verified that Si becomes metallic when the dopant concentration increases (Figure S3 in the Supporting Information).

In accordance with the experimental conditions (HF-etched Si surface) used to elaborate the peptides via phage display, we considered a monohydride-terminated n^+-Si surface[41] to study peptide interactions; its geometry is presented in Figure 3. The parameters for Si−H were obtained from the literature[41−43] and incorporated into the CVFF force field. Such a model was already successfully used to study the interaction between water and a monohydrated Si surface.[44]

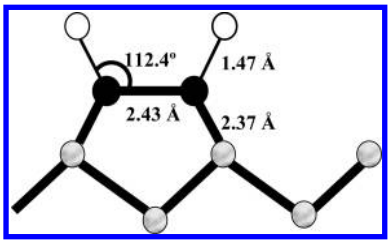

Figure 3. Geometry of the monohydride-terminated Si surface. White circles represent H atoms, and black and gray circles show the top-layer and bulk Si atoms, respectively.

Adsorption of Peptides on the Even n^+-Type Si(100) Surface in Vacuum. It has been demonstrated that in the vicinity of a surface, peptides susceptible to form multiple conformations adopt new favorable configurations enabling their binding to the surface.[19,33] Therefore, for binding energy calculations we placed solvated peptides at a distance of 5 Å away from the surface. Computing time limitations prevented us from testing all possible orientations of the peptide with respect to substrate. Hence, to obtain substantial results to understand the trajectory of peptide on the surface, 12 different initial configurations obtained by 30° rotation of the peptide were tested. As shown in Figure 4b−d, all three peptides change their conformations to match the Si surface by adjusting their backbones and side chains. As an example, in the magnified **P1** structure presented in Figure 4a, the interactions of atoms making contact with the surface are indicated by dotted lines. Atoms approaching the surface at 2.5−3.2 Å indicate moderate electrostatic interactions; those at 3.2−4.0 Å correspond to weak electrostatic interactions.[45] The sulfur atom in **P1** (Figure 4a) approaches the surface as close as 3 Å, strongly contributing to binding of peptide **P1** to the surface. Figure 4c shows that the atoms of **P2** match the substrate better and form more interactions compared with peptides **P1** and **P3** (Figure 4b,d).

The optimal peptide structure is determined by comparing the binding energies of different conformations to the n^+-Si surface, calculated as the difference between the average energy of the Si semiconductor−peptide system and the sum of the individual energies of the semiconductor and the peptide:

$$E_{\text{binding}} = E_{\text{semiconductor+peptide}} - (E_{\text{semiconductor}} + E_{\text{peptide}}) \quad (1)$$

Table 2 gathers the calculated binding energies of peptides toward the n^+-Si surface as well as the apparition frequencies of the three peptides when elaborated by phage display.[22] As indicated, **P2** binds more strongly to the n^+-Si surface than **P1**

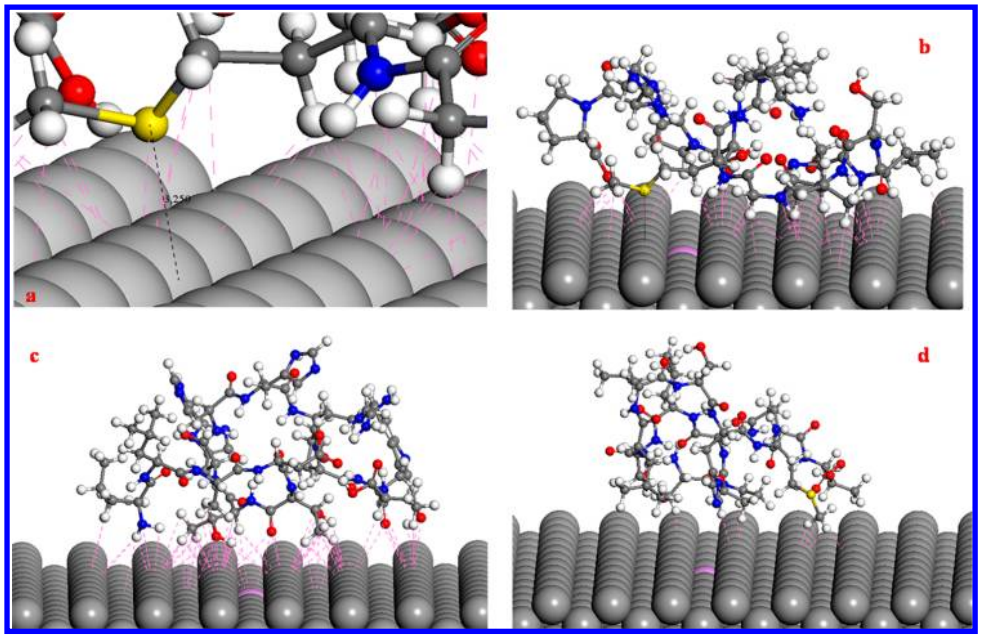

Figure 4. Comparison of molecular arrangements of peptides (b) **P1** (SVSVGMKPSPRP), (c) **P2** (LLADTTHHRPWT), and (d) **P3** (SPGLSVSHMQT) on the n^+-type silicon surface. (a) Magnified picture of **P1** to reveal the nearest atoms and their interactions (dotted lines) with n^+-Si.

Table 2. Phage Display Apparition Frequencies and Average Binding Energies of Peptides on the n^+-Si(100) Surface in Vacuum

peptide	apparition frequency	$E_{binding}$ (kcal/mol)[a]
SVSVGMKPSPRP (**P1**)	44%	−11.52 ± 1.47
LLADTTHHRPWT (**P2**)	28.5%	−14.53 ± 0.91
SPGLSLVSHMQT (**P3**)	44.4%	−7.01 ± 1.76

[a]Average ± standard deviation.

and **P3** and exhibits similar behavior for both conformations, providing an easy choice for computation in explicit solvents. This result corroborates our previous experimental work where **P2** was identified as an n^+-Si specific peptide.[22] Although peptide **P1** was recovered at a high frequency from the phage display technique, it has a lower binding energy toward the n^+-Si surface than **P2**. This is in good agreement with previous reports stating that **P1** is a thermodynamically unstable peptide (see Table 1) that is overexpressed in the phage display as a result of its high amplification potential rather than a real material-specific adhesion peptide.[46,47] As **P1** is often selected against various

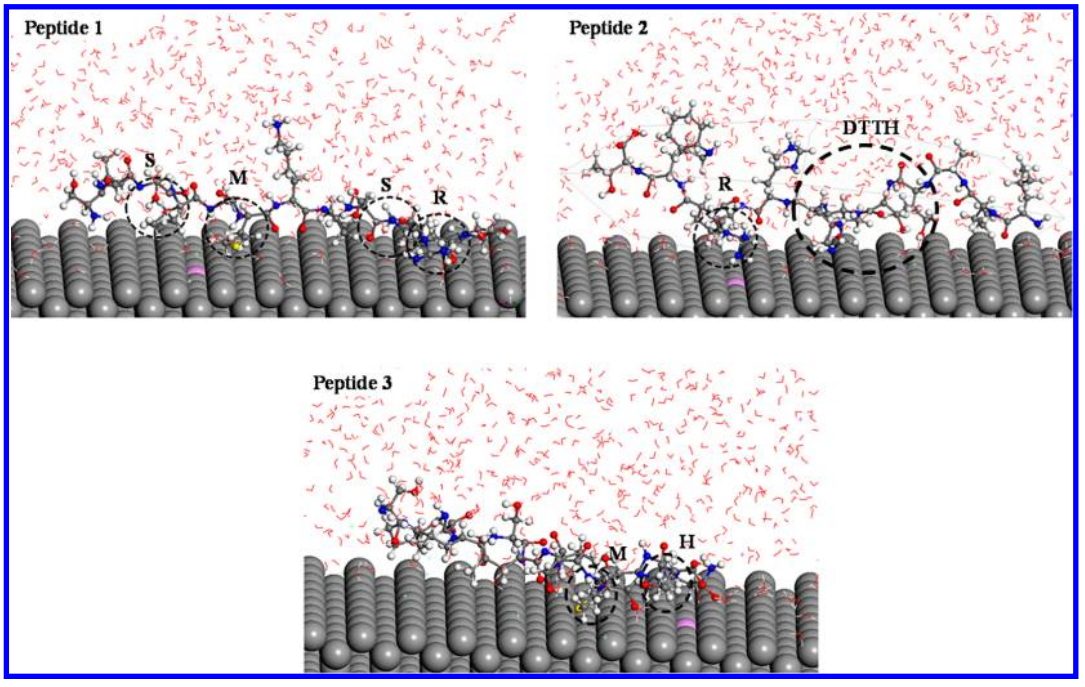

Figure 5. MD snapshots (side views) of peptides **P1**−**P3** on the n^+-Si surface in explicit solvent with buffering ions (137 mM PBS, pH 7).

dx.doi.org/10.1021/ci500260v | J. Chem. Inf. Model. 2014, 54, 2117−2126

organic and inorganic targets,[15,48] we avoid its use as a Si-specific peptide.[22] The low binding energy observed for peptide **P3** toward n^+-Si is not surprising in view of the fact that this peptide is a high-affinity linker for p^+-type Si[22] and was selected here as a negative control peptide for the n^+-type Si.

Adsorption of Peptides on the n^+-Type Si(100) Surface in Explicit Solvent. Under real experimental conditions, peptide adsorption occurs in a liquid environment, where modifications of the peptide conformation due to the presence of water molecules and ions are expected.[18] Therefore, to mimic the experimental conditions (i.e., 137 mM PBS), in our calculations peptides were placed in 12 different configurations in a solvent box containing ionic solute to obtain a reasonable sampling without being computationally too expensive. An interfacial water layer was considered between the surface and the solvated peptides, and the peptides were allowed to evolve for 100 ns on the Si surface. The final configurations of the peptides close to the n^+-Si surface are depicted in Figure 5. The folding and reorganization of the three peptides while they approach the surface are well-illustrated in movies 1−3 in the Supporting Information. It should be noted that peptide **P3**, which is not specific for n^+-Si, shows a tendency to fold in a globular configuration rather to align against the surface, contrary to peptides **P1** and **P2**, which readily adsorb in a relatively open structure. Adsorption of the peptides was quantified by monitoring the decrease in the potential energy of the system during the simulations (Figure S4 in the Supporting Information). We also identified the strongly binding amino acids versus the weaker-binding ones by comparing their distances from the surface and the forces of their attraction. Among the several configurations, we considered only the peptide with highest binding energy toward the surface for analysis. The amino acids and sequences nearest to the n^+-Si surface within the three peptides **P1**−**P3** are encircled in the configurations represented in Figure 5 and are indicated in Table 3.

Table 3. Amino Acids Nearest to the n^+-Si(001) Surface (Italicized and Underlined) As Obtained from MD Simulations of the Adsorption of Peptides P1−P3 in Explicit Solvent

peptide	peptide sequence
P1	SV*S*VG*M*KP*S*P*R*P
P2	LLA*DTTH*H*R*PWT
P3	SPGLSLVS*HM*QT

We can distinguish stronger-binding versus weaker-binding peptides from the plot of the MD trajectories of the peptides' adsorption energies over time (Figure 6). These energies were calculated according to the equation[24]

$$E_{ads} = E_1 - E_2 + E_3 - E_4 \quad (2)$$

where E_1, E_2, E_3 and E_4 are the average energies of the surface−amino acid−solvent system, the amino acid−solvent system, the solvent system, and the surface−solvent system, respectively. The obtained adsorption energies range from −10 to −30 kcal/mol. The data plotted here represent the trajectories of the best-binding peptide configurations toward the surface.

P2 peptide binds to the surface more strongly than **P1** and **P3**, which are rather unstable peptides (see the instability indices in Table 1). This is in good agreement with previous experimental results, where **P2** was found to be the best adhesion peptide for

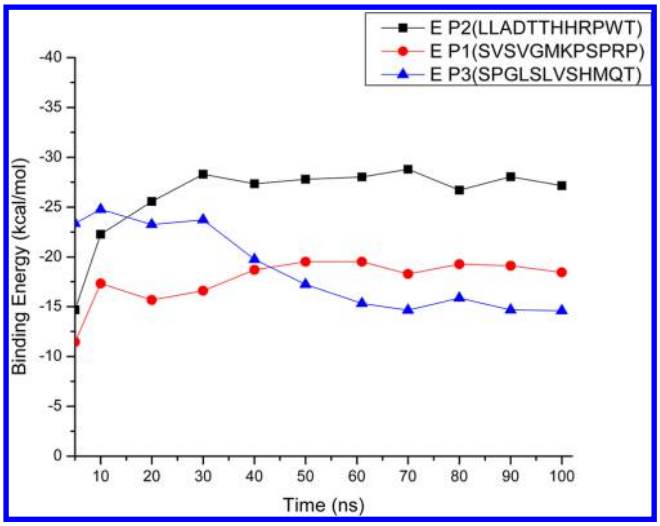

Figure 6. Computed binding energies of peptides **P1**−**P3** in aqueous ionic solution.

n^+-Si.[22,49] Even though **P1** has a high net positive charge (see Table 1), this peptide binds less strongly to the n^+-Si surface. The adsorption kinetics of **P3** shows a decreasing trend, probably because **P3** is more hydrophobic than **P1** and **P2**. The lack of affinity of **P3** for n^+-Si is evident when we consider that in the simulations peptides **P1** and **P2** were placed 5 Å from the surface, whereas **P3** was placed 3 Å from the surface.

Peptides **P1** and **P2** contain higher numbers of strongly binding amino acid residues, conferring upon them stronger adsorption onto n^+-Si. Peptide **P3** has only a few binding residues, and thus, its interaction with the surface is weaker. Our calculations also indicate that adsorption of **P2** is stronger compared with **P1** even though its apparition frequency in phage display is lower. The strongest-binding fragments of the peptide **P2** are the arginine (R) and a stretch of four polar amino acids (DTTH), whereas in peptides **P1** and **P3** only individual amino acids (S, M, R and H, M, respectively) were identified to make direct contact with the surface. Though S greatly contributes to **P1** binding, it does not play the same role when present in **P3**. On the contrary, R and M residues are identified as the best binders in two peptides: R in **P1** and **P2** and M **P1** and **P3**. This suggests that the role of the identities of individual amino acids and their associated characteristics in driving the adsorption of peptides is at least controversial. The importance of the identity of amino acids in the peptide cannot be denied; however, their place in the sequence seems to be important, too. To address this issue, we further carried out simulations with modified peptide sequences.

As we found that the methionine residue created direct contact with the n^+-Si surface to enable binding of the unspecific peptides (**P1** and **P3**), we decided to include M in the sequence of **P2** to enhance the already high binding affinity of this peptide toward n^+-Si. To scan the role of the amino acid identity and its location in the sequence, 12 mutants of peptide **P2** (LLADTTHHRPWT) were created by successively replacing one of the 12 amino acids with M (Figure 7). We quantified the binding of the mutants by calculating their residual activities, defined as the percentage of the binding energy of the mutant with respect to that of the wild-type peptide. The substitution of proline with methionine (the 10th **P2** mutant) enhanced the binding of the peptide to the n^+-Si surface by nearly 50%. On the contrary, the substitutions of tryptophan (the 11th **P2** mutant) and threonine (the 12th **P2** mutant) by methionine dramatically

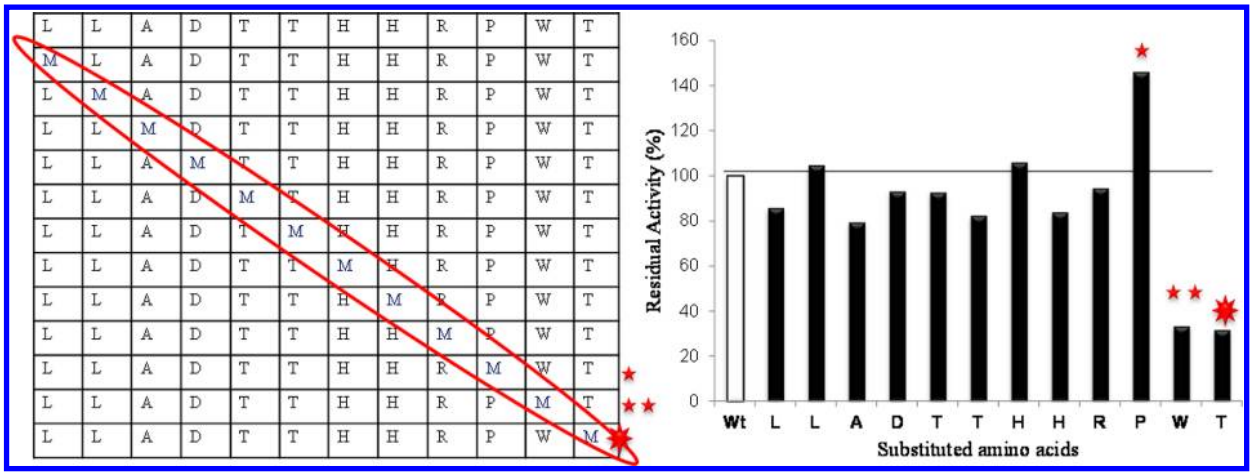

Figure 7. Activities of the methionine mutants of peptide **P2** (shown in the table) in terms of surface adhesion calculated by MD simulations. The mutants were obtained by replacing one amino acid in the wild type (Wt) peptide **P2** with methionine (M) in explicit solvent (same conditions). The values are given as the percentage of the binding energy of the mutant with respect to that of the Wt peptide. Symbols (stars) are for illustration purposes to relate the sequence and its residual activity.

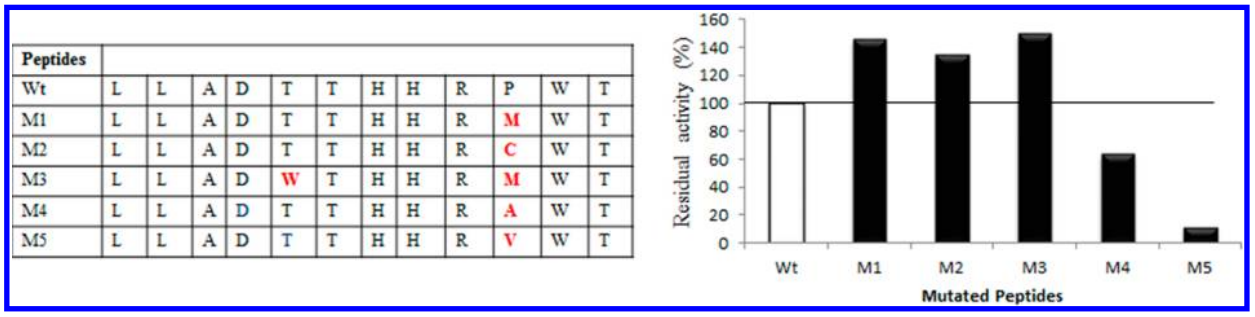

Figure 8. Effect of aliphatic and aromatic substitutions on the binding activity of peptide **P2** as determined by MD simulations (Wt, wild-type **P2**; M1−5, mutated peptides as shown in the table). Activity values are given as the percentage of binding energy of the peptide mutant with respect to that of the wild -type peptide **P2**.

reduced the strength of peptide binding to the surface. This indicates the crucial role of threonine and tryptophan in the binding affinity of **P2** toward n^+-Si. The T and W residues, which are different in nature (T is polar and W aromatic nonpolar), were not identified as best binders in **P2** (Table 3); however, their presence in the peptide sequence might be decisive for the optimal configuration adopted by **P2** close to the surface.

To investigate the effect of aliphatic and aromatic residues on the binding activity of **P2** on n^+-Si, we created five mutated peptides of **P2**. Four one-point mutants (M1, M2, M4, and M5) were obtained by successively replacing proline (P) with methionine (M), cysteine (C), alanine (A) and valine (V), respectively. In one double-mutant peptide (M3), threonine (T) was changed to tryptophan (W) and proline (P) to methionine (M). The calculated binding activities of the mutants are compared to that of wild-type **P2** in Figure 8. As observed before, replacing P with M enhances the binding activity (146% for the M1 mutant). The affinity is also enhanced when P is replaced by C (135% for the M2 mutant), though to a lesser extent, certainly because of the presence of S atom that binds strongly to n^+-Si. The double-mutant peptide M3 reveals the highest binding activity (150%), pointing out the importance of the presence of W. On the contrary, the substitution of P with A (M4) or V (M5) dramatically reduces the affinity of the mutated peptide for n^+-Si.

CONCLUSIONS

The objective of our work was to investigate the molecular mechanism underlying the strong binding of adhesion peptides to silicon. This work complements numerous recent studies focused on peptides' adsorption onto metals and metal oxides. Up to now, because of the lack of accurate force-field parameters for Si, theoretical calculations of the interactions between Si surfaces and peptides have been missing.

We studied the adsorption on silicon of three 12-mer peptides that were previously elaborated by phage display technology. P-doped n^+-type Si was modeled by DFT, and CVFF was parametrized for n^+-Si. Random-coil and local-minimum conformations of the peptides were generated, and their interaction with the n^+-type Si was studied. MD simulations were performed to monitor the organization of the peptides on the n^+-Si surface and to identify the atoms creating the strongest interactions (when the atom−surface distance was shorter than 4 Å) and the amino acid residues that are closest to the surface. Adsorption energy calculations confirmed the experimentally observed preferential adsorption of the peptides **P1** (SVSVGMKPSPRP) and **P2** (LLADTTHHRPWT) on n^+-Si relative to peptide **P3** (SPGLSLVSHMQT), which has been selected against the p^+-Si material.

The selectivity and binding affinity rely on both the peptide composition and the amino acid sequence. Our residual scanning analysis indicated that substituting proline by methionine in the sequence of **P2** enhances its affinity, whereas mutating

dx.doi.org/10.1021/ci500260v | J. Chem. Inf. Model. 2014, 54, 2117−2126

tryptophan or threonine with M totally destroys it. This indicates the essential role of threonine and tryptophan in the affinity of **P2** for n^+-Si. The double mutant containing M and W instead of P and T, respectively, reveals an enhanced binding affinity compared with wild-type **P2**. The presence of residues containing a sulfur atom, such as methionine (M) and cysteine (C), largely contribute to the peptide−Si interactions.

Summarizing, we have shown that the best-binding residues within the **P2** (LLADTTHHRPWT) peptide are polar D, T, H, and R and nonpolar aromatic W. Introducing M, C, and additional W in the **P2** sequence enhances its binding affinity for n^+-Si, whereas the presence of short nonpolar residues (e.g., A and V) destroys this affinity. Therefore, we have shown that both the amino acid sequence and the molecular architecture of the peptide are key determinants for the selective binding of peptides onto Si.

To our knowledge, the presented work reveals for the first time the interactions of peptides with hydride-terminated silicon. Although we are aware that our results are limited by the accuracy of the force fields, the computational time, and the conformational sampling of the peptides, the MD simulations still proved to be suitable to explain the differential adsorption of peptides onto Si that was previously observed experimentally. Future models can be developed employing other force fields and alternative MD methods.

COMPUTATIONAL DETAILS

Computation of Peptide Structure. Atomistic models of peptides were built in Discovery Studio Visualizer 3.5. With the conformation generation module in the Hyperchem molecular modeling program,[38] the lowest-energy conformation was chosen as the local-minimum conformation by variation of dihedral angles randomly out of several conformations. For each peptide, the maximum number of conformers to be generated was set to 1000. The energy of the modeled peptide structure was minimized under explicit-solvent conditions using CHARMM 27 force field parameters. The structure was verified for any main- or side-chain conformation violation. The protein secondary structure prediction program SOPMA[50] indicated that the peptides bear predominantly a random-coil structure.

n^+-Si Surface Simulation Using DFT Calculations. The first-principles calculations were performed within the DFT framework using the plane-wave pseudopotential method to cross-validate the heavily doped n^+-type Si surface with the experimentally prepared surface. For these calculations, the CASTEP module in Materials Studio was used.[51,52] The exchange−correlation effects were treated within the generalized gradient Perdew−Burke−Ernzerhof (PBE) functional correlation.[53] The energy cutoff was varied from 170 to 310 eV. The self-consistent field (SCF) convergence parameters were set at 2×10^{-5} eV and the maximum stress component at 0.05 GPa. After geometry optimization, the band structure, density of states, and electron density were calculated.

Peptide Binding Simulation Protocol. To maintain physiological conditions, we added Na^+, Cl^-, and HPO_4^{2-} ions to the solvation box. The peptides were allowed to relax in solvent before being placed on the surface. The energy-minimized solvated peptides were then approached to the substrate in 12 configurations obtained by 30° rotations. We used the LAMMPS simulation package[54] and the Discovery program to run MD simulations. All of the simulations were performed under *NVT* ensemble conditions at 300 K. The periodic box dimensions were typically 4 nm × 3 nm × 1.5 nm for the silicon surface. The periodic box dimensions for systems containing peptide, solution, and surface were set to 4 nm × 3 nm × 4.5 nm to allow the accommodation of large numbers of water molecules and buffering ions. The consistent valence force field (CVFF)[55] parametrized accurately with silicon parameters[41−43] (Table 4)

Table 4. Force Field Parameter Values (r is the Bond Length and Θ is the Bond Angle)

group type	parameter value
r_{Si-H}	1.47 Å
r_{Si-Si}	2.37 Å
$\Theta_{H-Si-Si}$	112.4°

was used for the surface, the protein, and the buffering ions. The TIP3P model was used for water. The total potential energy of the system was calculated as the sum of the energies due to Coulombic, van der Waals, and bonded (stretching/angular) interactions:

$$U_{total} = U_{Coul} + U_{vdW} + U_{bond} + U_{angle} \quad (3)$$

Computation of Binding Energies. To compute binding energies, MD simulations were carried out in vacuum and under explicit-solvent conditions. We used the four systems approach to quantitatively compute binding energies in explicit solvent.[24] All of the simulations were run for 100 ns. The final adsorption energy was calculated by taking the uncertainty of the Coulombic interactions (≤0.01 kcal/mol) into account. Adsorption energy values and atomic coordinates were collected every 5 ps.

ASSOCIATED CONTENT

Supporting Information

Supplementary figures and movies (AVI). This material is available free of charge via the Internet at http://pubs.acs.org.

AUTHOR INFORMATION

Corresponding Author

*E-mail: Csilla.gergely@univ-montp2.fr.

Notes

The authors declare no competing financial interest.

ACKNOWLEDGMENTS

We thank Frédéric J. G. Cuisinier for his support to carry out the computations. We are thankful for the support of computational resources provided by Centre Informatique National de l'Enseignement Supérieur (CINES).

ABBREVIATIONS

QM, quantum-mechanical; MD, molecular dynamics.

REFERENCES

(1) Busch, S. Regeneration of Human Tooth Enamel. *Angew. Chem., Int. Ed.* **2004**, *43*, 1428−1431.

(2) Lin, A. Y.; Chen, P. Y.; Meyers, M. A. The Growth of Nacre in the Abalone Shell. *Acta Biomater.* **2008**, *4*, 131−138.

(3) Alves, N. M.; Leonor, I. B.; Azevedo, H. S.; Reis, R. L.; Mano, J. F. Designing Biomaterials Based on Biomineralization of Bone. *J. Mater. Chem.* **2010**, *20*, 2911−2921.

(4) Niemeyer, C. M. Nanoparticles, Proteins, and Nucleic Acids: Biotechnology Meets Materials Science. *Angew. Chem., Int. Ed.* **2001**, *40*, 4128−4158.

(5) Pavan, S.; Berti, F. Short Peptides as Biosensor Transducers. *Anal. Bioanal. Chem.* **2012**, *402*, 3055−3070.

(6) Seeman, N. C.; Belcher, A. M. Emulating Biology: Building Nanostructures from the Bottom Up. *Proc. Natl. Acad. Sci. U.S.A.* **2002**, *99* (Suppl. 2), 6451−6455.
(7) Mannoor, M. S.; Zhang, S.; Link, A. J.; McAlpine, M. C. Electrical Detection of Pathogenic Bacteria via Immobilized Antimicrobial Peptides. *Proc. Natl. Acad. Sci. U.S.A* **2010**, *107*, 19207−19212.
(8) Brown, S. Metal-Recognition by Repeating Polypeptides. *Nat. Biotechnol.* **1997**, *15*, 269−272.
(9) Tamerler, C.; Sarikaya, M. Molecular Biomimetics: Utilizing Nature's Molecular Ways in Practical Engineering. *Acta Biomater.* **2007**, *3*, 289−299.
(10) Umetsu, M.; Mizuta, M.; Tsumoto, K.; Ohara, S.; Takami, S.; Watanabe, H.; Kumagai, I.; Adschiri, T. Bioassisted Room-Temperature Immobilization and Mineralization of Zinc Oxide—The Structural Ordering of ZnO Nanoparticles into a Flower-Type Morphology. *Adv. Mater.* **2005**, *17*, 2571−2575.
(11) Date, T.; Tanaka, K.; Nagamura, T.; Serizawa, T. Directional Affinity of Short Peptides for Synthetic Polymers. *Chem. Mater.* **2008**, *20*, 4536−4538.
(12) Wang, S.; Humphreys, E. S.; Chung, S. Y.; Delduco, D. F.; Lustig, S. R.; Wang, H.; Parker, K. N.; Rizzo, N. W.; Subramoney, S.; Chiang, Y. M.; Jagota, A. Peptides with Selective Affinity for Carbon Nanotubes. *Nat. Mater.* **2003**, *2*, 196−200.
(13) Estephan, E.; Larroque, C.; Cuisinier, F. J. G.; Bálint, Z.; Gergely, C. Tailoring GaN Semiconductor Surfaces with Biomolecules. *J. Phys. Chem. B* **2008**, *112*, 8799−8805.
(14) Whaley, S. R.; English, D. S.; Hu, E. L.; Barbara, P. F.; Belcher, A. M. Selection of Peptides with Semiconductor Binding Specificity for Directed Nanocrystal Assembly. *Nature* **2000**, *405*, 665−668.
(15) Estephan, E.; Larroque, C.; Bec, N.; Martineau, P.; Cuisinier, F. J.; Cloitre, T.; Gergely, C. Selection and Mass Spectrometry Characterization of Peptides Targeting Semiconductor Surfaces. *Biotechnol. Bioeng.* **2009**, *104*, 1121−1131.
(16) Estephan, E.; Saab, M.; Larroque, C.; Martin, M.; Olsson, F.; Lourdudoss, S.; Gergely, C. Peptides for Functionalization of InP Semiconductors. *J. Colloid Interface Sci.* **2009**, *337*, 358−363.
(17) Saab, M. B.; Estephan, E.; Cloitre, T.; Larroque, C.; Gergely, C. Peptide Route Functionalization of ZnSe Crystals Preserves Activity and Structure of Proteins While Adsorption. *J. Phys. Chem. C* **2010**, *114*, 18509−18515.
(18) McConnell, S. J.; Hoess, R. H. Tendamistat as a Scaffold for Conformationally Constrained Phage Peptide Libraries. *J. Mol. Biol.* **1995**, *250*, 460−470.
(19) Oren, E. E.; Tamerler, C.; Sarikaya, M. Metal Recognition of Septapeptides via Polypod Molecular Architecture. *Nano Lett.* **2005**, *5*, 415−419.
(20) Willett, R. L.; Baldwin, K. W.; West, K. W.; Pfeiffer, L. N. Differential Adhesion of Amino Acids to Inorganic Surfaces. *Proc. Natl. Acad. Sci. U.S.A.* **2005**, *102*, 7817−7822.
(21) Puddu, V.; Perry, C. C. Peptide Adsorption on Silica Nanoparticles: Evidence of Hydrophobic Interactions. *ACS Nano* **2012**, *6*, 6356−6363.
(22) Estephan, E.; Saab, M. B.; Agarwal, V.; Cuisinier, F. J. G.; Larroque, C.; Gergely, C. Peptides for the Biofunctionalization of Silicon for Use in Optical Sensing with Porous Silicon Microcavities. *Adv. Funct. Mater.* **2011**, *21*, 2003−2011.
(23) Di Felice, R.; Corni, S. Simulation of Peptide−Surface Recognition. *J. Phys. Chem. Lett.* **2011**, *2*, 1510−1519.
(24) Heinz, H.; Farmer, B. L.; Pandey, R. B.; Slocik, J. M.; Patnaik, S. S.; Pachter, R.; Naik, R. R. Nature of Molecular Interactions of Peptides with Gold, Palladium, and Pd−Au Bimetal Surfaces in Aqueous Solution. *J. Am. Chem. Soc.* **2009**, *131*, 9704−9714.
(25) Monti, S.; Carravetta, V.; Battocchio, C.; Iucci, G.; Polzonetti, G. Peptide/TiO_2 Surface Interaction: A Theoretical and Experimental Study on the Structure of Adsorbed Ala-Glu and Ala-Lys. *Langmuir* **2008**, *24*, 3205−3214.
(26) Hong, G.; Heinz, H.; Naik, R. R.; Farmer, B. L.; Pachter, R. Toward Understanding Amino Acid Adsorption at Metallic Interfaces: A Density Functional Theory Study. *ACS Appl. Mater. Interfaces* **2009**, *1*, 388−392.
(27) Iori, F.; Corni, S.; Di Felice, R. Unraveling the Interaction between Histidine Side Chain and the Au(111) Surface: A DFT Study. *J. Phys. Chem. C* **2008**, *112*, 13540−13545.
(28) Bent, S. F. Organic Functionalization of Group IV Semiconductor Surfaces: Principles, Examples, Applications, and Prospects. *Surf. Sci.* **2002**, *500*, 879−903.
(29) Buriak, J. M. High Surface Area Silicon Materials: Fundamentals and New Technology. *Philos. Trans. R. Soc., A* **2006**, *364*, 217−225.
(30) Brzoska, J. B.; Benazouz, I.; Rondelez, F. Silanization of Solid Substrates—A Step toward Reproducibility. *Langmuir* **1994**, *10*, 4367−4373.
(31) Ouyang, H.; Christophersen, M.; Viard, R.; Miller, B. L.; Fauchet, P. M. Macroporous Silicon Microcavities for Macromolecule Detection. *Adv. Funct. Mater.* **2005**, *15*, 1851−1859.
(32) Ramakrishnan, S. K.; Martin, M.; Cloitre, T.; Firlej, L.; Cuisinier, F. J.; Gergely, C. Insights on the Facet Specific Adsorption of Amino Acids and Peptides toward Platinum. *J. Chem. Inf. Model.* **2013**, *53*, 3273−3279.
(33) Verde, A. V.; Acres, J. M.; Maranas, J. K. Investigating the Specificity of Peptide Adsorption on Gold Using Molecular Dynamics Simulations. *Biomacromolecules* **2009**, *10*, 2118−2128.
(34) Emami, F. S.; Puddu, V.; Berry, R. J.; Varshney, V.; Patwardhan, S. V.; Perry, C. C.; Heinz, H. A Force Field and a Surface Model Database for Silica To Simulate Interfacial Properties in Atomic Resolution. *Chem. Mater.* **2014**, *26*, 2647−2658.
(35) Kyte, J.; Doolittle, R. F. A Simple Method for Displaying the Hydropathic Character of a Protein. *J. Mol. Biol.* **1982**, *157*, 105−132.
(36) Smith, R. L.; Collins, S. D. Porous Silicon Formation Mechanisms. *J. Appl. Phys.* **1992**, *71*.
(37) Gupta, P.; Colvin, V. L.; George, S. M. Hydrogen Desorption Kinetics from Monohydride and Dihydride Species on Silicon Surfaces. *Phys. Rev. B* **1988**, *37*, 8234−8243.
(38) *Hyperchem*, version 7.5; Hypercube, Inc.: Gainesville, FL, 2006.
(39) MacKerell, A. D.; Bashford, D.; Bellott, M.; Dunbrack, R. L.; Evanseck, J. D.; Field, M. J.; Fischer, S.; Gao, J.; Guo, H.; Ha, S.; Joseph-McCarthy, D.; Kuchnir, L.; Kuczera, K.; Lau, F. T. K.; Mattos, C.; Michnick, S.; Ngo, T.; Nguyen, D. T.; Prodhom, B.; Reiher, W. E.; Roux, B.; Schlenkrich, M.; Smith, J. C.; Stote, R.; Straub, J.; Watanabe, M.; Wiorkiewicz-Kuczera, J.; Yin, D.; Karplus, M. All-Atom Empirical Potential for Molecular Modeling and Dynamics Studies of Proteins. *J. Phys. Chem. B* **1998**, *102*, 3586−3616.
(40) Levine, Z. H.; Allan, D. C. Calculation of the Nonlinear Susceptibility for Optical Second-Harmonic Generation in III−V Semiconductors. *Phys. Rev. Lett.* **1991**, *66*, 41−44.
(41) Hansen, U.; Vogl, P. Hydrogen Passivation of Silicon Surfaces: A Classical Molecular-Dynamics Study. *Phys. Rev. B* **1998**, *57*, 13295−13304.
(42) Murty, M. R.; Atwater, H. A. Empirical Interatomic Potential for Si−H Interactions. *Phys. Rev. B* **1995**, *51*, 4889−4893.
(43) Gordon, M. S.; Truong, T. N.; Bonderson, E. K. Potential Primary Pyrolysis Processes for Disilane. *J. Am. Chem. Soc.* **1986**, *108*, 1421−1427.
(44) Ioanid, A.; Dieaconu, M.; Antohe, S. A Semiempirical Potential Model for H-Terminated Functionalized Surface of Porous Silicon. *Dig. J. Nanomater. Biostruct.* **2010**, *5*, 947−957.
(45) Jeffrey, G. A. *An Introduction to Hydrogen Bonding*; Oxford University Press: Oxford, U.K., 1997.
(46) Estephan, E.; Dao, J.; Saab, M.-B.; Panayotov, I.; Martin, M.; Larroque, C.; Gergely, C.; Cuisinier, F. J.; Levallois, B. SVSVGMKPSPRP: A Broad Range Adhesion Peptide. *Biomed. Technol. Eng.* **2012**, *57*, 481−489.
(47) Kolb, G.; Boiziau, C. Selection by Phage Display of Peptides Targeting the HIV-1 TAR Element. *RNA Biol.* **2005**, *2*, 28−33.
(48) Arnaiz, B.; Madrigal-Estebas, L.; Todryk, S.; James, T. C.; Doherty, D. G.; Bond, U. A Novel Method To Identify and Characterise Peptide Mimotopes of Heat Shock Protein 70-Associated Antigens. *J. Immune Based Ther. Vaccines* **2006**, *4*, 1−12.

(49) Ramakrishnan, S. K.; Estephan, E.; Martin, M.; Cloitre, T.; Gergely, C. Probing the Mechanism of Material Specific Peptides for Optical Biosensors. *Proc. SPIE* **2013**, *8765*, No. 87650A.
(50) Geourjon, C.; Deleage, G. SOPMA: Significant Improvements in Protein Secondary Structure Prediction by Consensus Prediction from Multiple Alignments. *Comput. Appl. Biosci.* **1995**, *11*, 681−684.
(51) *Materials Studio*, version 6.0; Accelrys: San Diego, CA, 2012.
(52) Segall, M. D.; Lindan, P. J. D.; Probert, M. J.; Pickard, C. J.; Hasnip, P. J.; Clark, S. J.; Payne, M. C. First-Principles Simulation: Ideas, Illustrations and the CASTEP Code. *J. Phys.: Condens. Matter* **2002**, *14*, 2717−2744.
(53) Perdew, J. P.; Burke, K.; Ernzerhof, M. Generalized Gradient Approximation Made Simple. *Phys. Rev. Lett.* **1996**, *77*, 3865−3868.
(54) Plimpton, S. Fast Parallel Algorithms for Short-Range Molecular-Dynamics. *J. Comput. Phys.* **1995**, *117*, 1−19.
(55) Dauber-Osguthorpe, P.; Roberts, V. A.; Osguthorpe, D. J.; Wolff, J.; Genest, M.; Hagler, A. T. Structure and Energetics of Ligand Binding to Proteins: *Escherichia coli* Dihydrofolate Reductase−Trimethoprim, a Drug−Receptor System. *Proteins* **1988**, *4*, 31−47.